АКУСТОЕЛЕКТРОННІ СЕНСОРИ

ACOUSTOELECTRONIC SENSORS

PACS 07.07.Df, 02.70.Dh

FEATURES OF MICRON-SIZED MESA-PIEZORESISTOR

Victor A. Gridchin, Michail A. Chebanov

Novosibirsk State Technical University, Novosibirsk, Russia

FEATURES OF MICRON-SIZED MESA-PIEZORESISTOR

Victor A. Gridchin, Michail A. Chebanov

Abstract. The effect of dihedral angles in the junction region of tensoresistive layer to contact pads on strain distribution in mesa-piezoresistor body was studied using the finite element method. Influence of mesa-piezoresistor geometry on its sensitivity was demonstrated.

Keywords: Finite element method, pressure sensor, mesa-piezoresistor, mechanical stress concentrator

ОСОБЛИВОСТІ ДЕФОРМАЦІЇ МЕЗАТЕНЗОРЕЗИСТОРІВ МІКРОННИХ РОЗМІРІВ

Віктор А. Грідчін, Михайло А. Чебанов

Анотація. Використовуючи техніку кінцево-елементного моделювання, досліджено вплив двогранних кутів в області переходу тензорезистивного шару до контактних площадок на розподіл деформацій у тілі мезатензорезистора. Показано вплив геометричних розмірів мезатензорезисторів на їхню чутливість.

Ключові слова: кінцево-елементне моделювання, сенсор тиску, мезатензорезистор, концентратор механічних напруг

ОСОБЕННОСТИ ДЕФОРМАЦИИ МЕЗАТЕНЗОРЕЗИСТОРОВ МИКРОННЫХ РАЗМЕРОВ

Виктор А. Гридчин, Михаил А. Чебанов

Аннотация. Используя технику конечно-элементного моделирования, исследовано влияние двугранных углов в области перехода тензорезистивного слоя к контактным площадкам на распределение деформаций в теле мезатензорезистора. Показано влияние геометрических размеров мезатензорезисторов на их чувствительность.

Ключевые слова: конечно-элементное моделирование, сенсор давления, мезатензорезистор, концентратор механических напряжений

I. Introduction

Silicon-insulator-silicon (SIS) structures are becoming increasingly important for microsystem technology (MST) due to stricter requirements to sensors and expansion of high-temperature electronics market. According to expert assessment, this market will grow in average by 15% per annum till 2011 [1]. SIS structures are especially attractive for design of pressure sensors with temperature range up to 300°C. This is because SIS structures are cheap and available as compared with wide-gap semiconductors (SiC, C, GaAs). In SIS structures dielectric insulation is provided with SiO_2 layer, which has well studied properties and proven production techniques.

II. Problem definition

SIS structure piezoresistor are based on the mesa structure (Fig. 1), to which silicon resilient member transfers deformation through dielectric layer. Deformation field of the mesa-piezoresistor differs from the similar field of integrated piezoresistor with insulating p-n junction. This issue was earlier studied using the simple analytical model developed in papers [2] — [6]. The analysis was carried out for the simplified mesa-piezoresistor with rectangular parallelepiped shape with free faces, except for base (SiO_2-Si interface). That simple model allowed estimating geometry effects on longitudinal and transverse piezoresistor sensitivity.

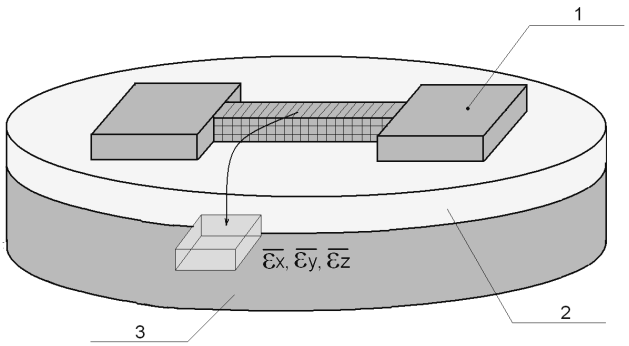

Fig. 1. Mesa-piezoresistor structure. 1 — polysilicon; 2 — dielectric; 3 — silicon

The real piezoresistor has more complex geometry and contains wide contact pads, and passivating layer covers not only top, but also side piezoresistor faces. The analytical solution cannot be obtained due to three-dimensionality of the structure. This paper presents the numerical model of mesa-piezoresistor; effects of longitudinal and lateral sizes on general piezoresistor deformation was analyzed using this model. Due to practical importance, special attention is paid to deformation of mesa-piezoresistor with micron lateral sizes.

III. Numerical model of mesa-piezoresistor

The mesa-piezoresistor structure determines the specific character of its strained state as compared with integrated piezoresistors. Mesa-structure deformation depends both on its shape and on piezoresistor size.

In this paper the quantitative analysis of strained state was carried out using the ANSYS program package (version 11). The structure is symmetrical; therefore only a quarter of the structure was analyzed (Fig. 2). The boundary conditions were specified as shift constraints shown in Fig. 2 for planes perpendicular to intrinsic directions. Such boundary conditions allow the structure to freely stretch and shrink along the axial directions. When calculating the resilient member was supposed to be uniaxially stretched away from the mesa-piezoresistor with load T_0.

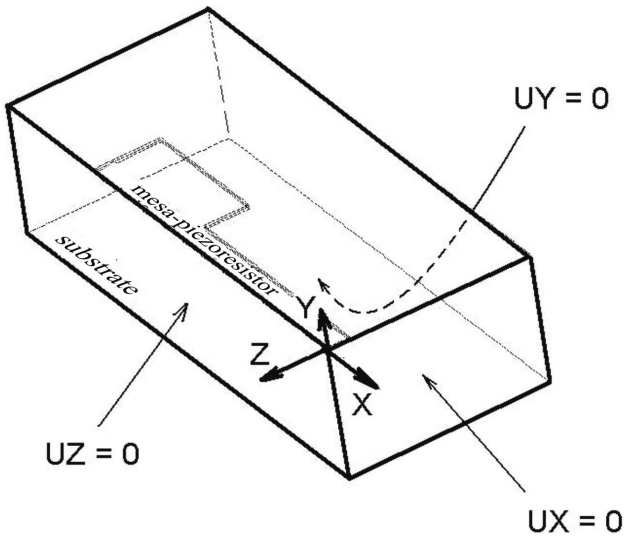

Fig. 2. The ways of boundary conditions settings

The structure was simulated with first-order finite element SOLID185, which is intended for three-dimensional solid-state structures and allows setting elastic properties of material through full matrix of elastic constants. Fig. 3 shows an example of the finite element model.

The structure simulation gives strained state of the mesa-piezoresistor. The next step was calculating of averaged values of strain components along

piezoresistor length for lower, middle and upper part. To solve the problem piezoresistor body was divided into sections (Fig. 1). An averaged value of strain component was numerically calculated for every section.

$$\overline{\varepsilon}_i = \frac{1}{V}\int_V \varepsilon_i(x,y,z)dV.$$

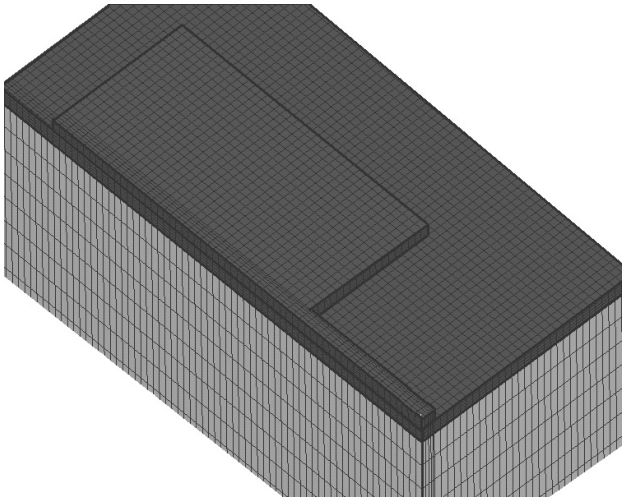

Fig. 3. Segment of finite-element structure model.

The integral calculation algorithm was realized by means of ANSYS programming (APDL language)

IV. Simulation results

Polysilicon piezoresistors with thickness h = 0.5 μm and width from 1 to 10 μm were simulated. A number of tensoresistive region squares was invariable in all cases (n = 10), so that tensoresistive region length was equal to $L = 10 \cdot w$. Contact pads have sizes from 10 μm for resistor with thickness w = 1 μm to 30 μm for resistor with thickness w = 10 μm. In the course of simulation thickness of the isolating SiO_2 layer was selected at 0.5 μm, and thickness of the silicon resilient member was equal to 40 μm. Resilient member ((100) plane) was uniaxially loaded along [100] direction, so that away from piezoresistor longitudinal strain was equal to $1 \cdot 10^{-3}$. Any other stresses were not taken into account in the SIS structure; therefore, effects of shape and size on piezoresistor deformation could be explicitly determined.

Fig. 4 and 5 show distribution of mean longitudinal strain along piezoresistor length for upper, middle and lower third parts of its thickness. Piezoresistor width was equal to 1 μm and 10 μm, respectively. Strain was averaged by volume $V_i = \frac{h}{3} \times \frac{w}{2} \times \frac{L}{20}$.

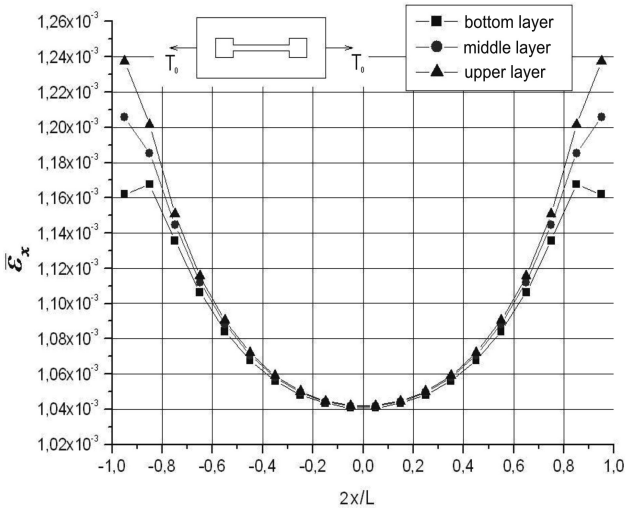

Fig. 4. Distribution of mean longitudinal strain along normalized piezoresistor body length (w = 1 μm)

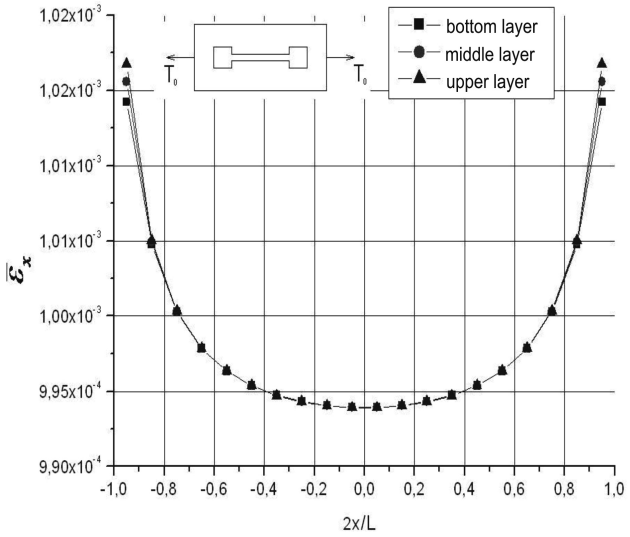

Fig. 5. Distribution of mean longitudinal strain along normalized piezoresistor body length (w = 10 μm)

The figures demonstrate that longitudinal strain distribution is almost uniform in thickness, except for edge areas, in which the narrow part of mesa-piezoresistors changes to a contact pad. Under the most unfavorable conditions (w = 1 μm) nonuniformity by thickness does not exceed 6%. The effect of piezoresistor width on longitudinal strain distribution over its length is stronger. This distribution has U-shape. The narrower piezoresistor, the stronger strain growth as approaching to contact pads. When width w = 10 μm longitudinal strain increase near tensoresistive region edges

equals to 2%, and when width w = 1 μm it equals to 24%.

Ratio of strain in piezoresistor centre $\delta = \frac{\overline{\varepsilon}_x(x=0)}{\varepsilon_{wafer}}$ to silicon resilient member strain $\varepsilon_{wafer} = 1 \cdot 10^{-3}$ is equal to $\delta = 0.97$ when w = 10 μm and to $\delta = 1.04$ when w = 1 μm.

Lateral strain of the mesa-piezoresistor is substantially smaller than resilient member strain. Decreasing degree depends not only on width, but also on distance between layer and piezoresistor base.

Fig. 6 and 7 show distribution of mean lateral strain $\overline{\varepsilon}_z$ in lower, middle and upper parts of the piezoresistor along its length. Even at piezoresistor width w = 10 μm strains are equal to 68%, 63% and 59% of resilient member strain, respectively. When w = 1 μm layer strains are equal 26%, 0.5% and -0.5%, respectively, and for the upper layer strain sign is reversed.

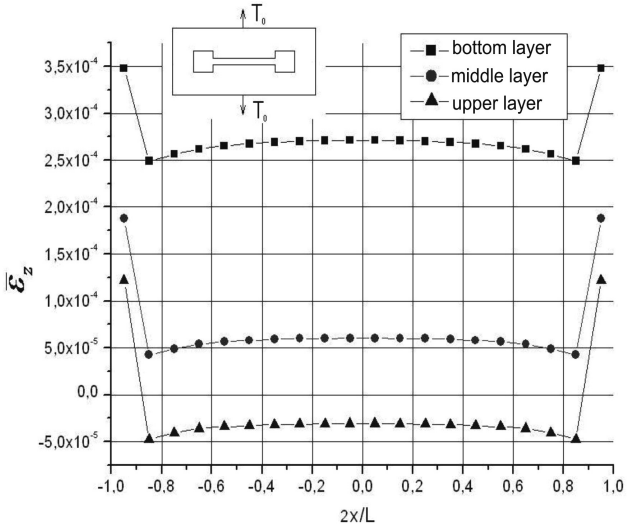

Fig. 6. Distribution of mean lateral strain along normalized piezoresistor body length (w = 1 μm)

It follows from shift stresses occurring on free side faces of the piezoresistor. Junction between tensoresistive part and contact pad remove such a degree of freedom and strains acquire right sign and grow in value. Such a transition is sufficient only for near-contact pad layers. Along the main body of mesa-piezoresistor lateral strain distribution is almost uniform.

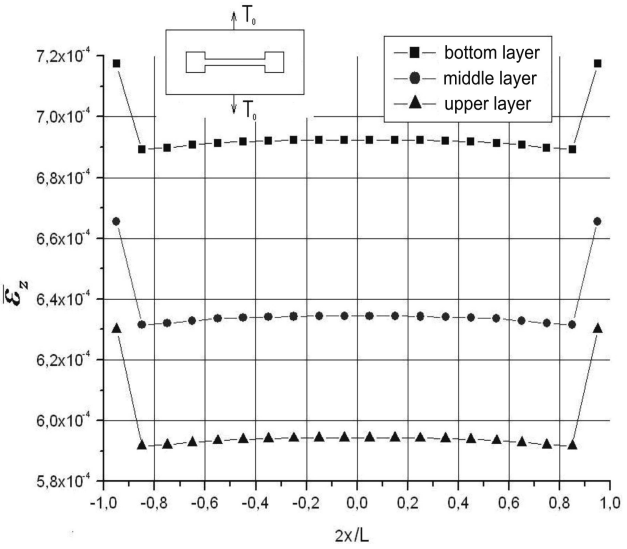

Fig. 7. Distribution of mean lateral strain along normalized piezoresistor body length (w = 10 μm)

V. Discussion of results

The existing techniques for estimation of integrated mesa-piezoresistor deformation are based on glued piezoresistor models [2, 6]. Piezoresistor is supposed to have the shape of rectangular parallelepiped with only base fixed and free faces. Then, strain distribution over cross section of such a piezoresistor is defined by [4]:

$$\varepsilon_x = \varepsilon_{x0}\left[1 - \frac{3y}{2h}\frac{ch(\lambda x)}{ch(\lambda a)}\right], \quad \varepsilon_z = \varepsilon_{z0}\left[1 - \frac{3y}{2h}\frac{ch(\lambda z)}{ch(\lambda a)}\right], \tag{1}$$

where $\varepsilon_x, \varepsilon_z$ is piezoresistor base strain (y = 0),

$$\lambda = \frac{1}{h}\sqrt{\frac{3}{2(1+\nu)}},$$

ν and h is Poisson's ratio of piezoresistor material and its thickness $2a = L$ or $2a = w$ at consideration of longitudinal or lateral strains. According to (1) strains sharply decrease when approaching to free faces, which allows qualitative explanation of sharp fall in transverse sensitivity of the piezoresistor in micro- and nanoscale.

Stress concentration near angles also effects on lateral piezoresistor deformation, but as soon as piezoresistor width is much smaller than its length $\left(w = \frac{1}{10}L\right)$, the role of angles is not so significant

and is observable only when approaching to contact pads.

Integrated mesa-piezoresistors have the shape that sufficiently differs from rectangular parallelepiped. Dihedral angles at contact pad junctions are stress concentrators, and the narrower piezoresistor is, the more important their role is. Fig. 8 shows strain ε_x distribution along $z = 0$ and $z = \frac{w}{2}$ lines along piezoresistor surface with thickness $w = 1$ μm. At junction between tensoresistive layer and contact pad longitudinal strain increases and rises when approaching to piezoresistor edge. At free contact pad face strains behave in accordance to (1) and drops to zero. For wide piezoresistors the role of dihedral angles drops, which can be seen when comparing Fig. 4 and 5.

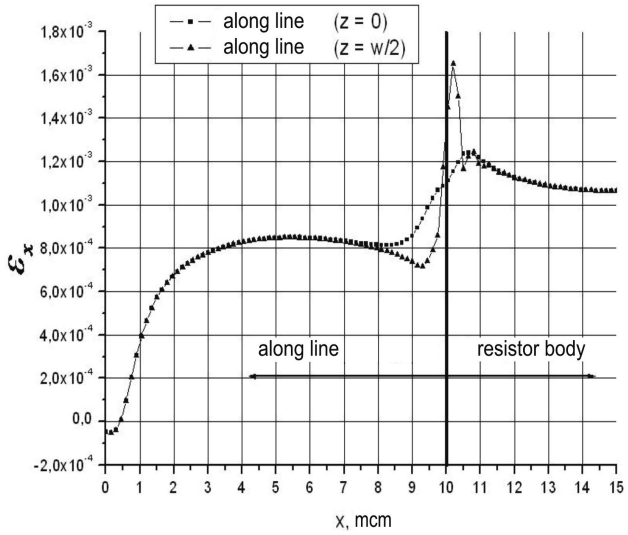

Fig. 8. ε_x component distribution over resistor surface for $z = 0$ and $z = w/2$

Local stresses near dihedral angles sufficiently effect on tensoresistive units strength; we published these findings earlier [7].

Features of strain distribution along and across piezoresistor effect on its tensoresistive properties. Change in resistance of longitudinal and lateral piezoresistors under uniaxial load are defined by expressions:

$$\frac{\Delta R}{R_0} = \pi_l \cdot \frac{1}{L}\int_0^L \overline{T}_x(x)dx, \frac{\Delta R}{R_0} = \pi_t \cdot \frac{1}{L}\int_0^L \overline{T}_z(x)dx,$$

where π_l and π_t are longitudinal and lateral piezoresistance factors, respectively.

Determination of averaged stress values $\overline{T}_x$ and $\overline{T}_z$ is not a simple task. In this study $\overline{T}_i$ value was defined through averaging by upper, middle and lower piezoresistor volumes V_i of the piezoresistor. The calculation results based on this technique are given in Fig. 9. The simulation shows that decrease in width of the mesa-piezoresistors results in decrease in their transverse sensitivity and increase in longitudinal one. Transverse sensitivity decrease was experimentally confirmed for mesa-piezoresistors with width-thickness ratio in the range $16 \le w/h \le 200$ [8].

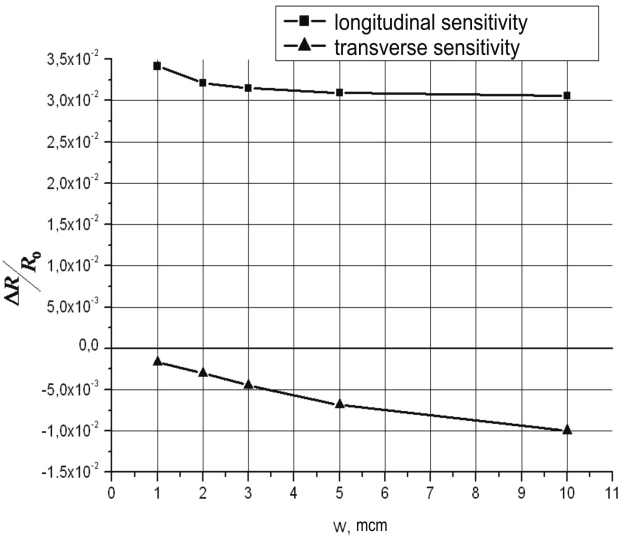

Fig. 9. Distribution of transverse and longitudinal sensitivity on width of mesa-piezoresistor

When $w/h = 16$ transverse sensitivity decrease is about 25%. In this study w/h ratio is significantly smaller, $2 \le w/h \le 20$ and, therefore, more sufficient transverse sensitivity decrease is observed (Fig. 9).

Increase in longitudinal sensitivity of the mesa-piezoresistor with thickness of about 1 μm and length $L \approx 10$ μm was not studied experimentally up to now. The available experimental data [8] were obtained for large structures ($L > 117$ μm, $w \ge 7.9$ μm), when geometric effects are not observable. The longitudinal piezoresistivity increase observed in nanostructures [9] is attributed to energy spectrum change, rather than to geometry effect (in paper [9] $L/h \approx 60$).

The numerical simulation results show that additional longitudinal piezoresistivity increase may occur in short nanostructures due to geometry effects.

VI. Conclusion

The finite element modeling of mesa-piezoresistor demonstrates that its mean strains depend not only on its size, but also on its shape. Taking into account the effect of contact pads shows that for bone-like piezoresistor longitudinal strain may increase, while lateral strain may decrease. The sufficient role of dihedral angles at contact junctions as stress concentrators was demonstrated. This can result in additional longitudinal sensitivity increase for short mesa-piezoresistor in nanometer range.

This article supported: Program of fundamental scientific research ONIT RAS — project № 4.1 «Researching ways of construction and creation high temperature pressure sensors based on submicrometer and nanosized silicon structures on dielectric».

References

1. Jonston C. Electronics and Microsystems for high Temperatures — Markets and Applications, MST-news, 2001, №4/01, p. 4–5.
2. Seryoznov A. N., Skotnikov A. A., Prisekin V. L. Semiconductor Piezoresistor Errors Conditioned with Glue Layer Thickness. // Semiconductor Strain Gauging. Materials of IVth Conference on Semiconductor Strain Gauging, 22–27.09, 199, Lvov, 1971, pp. 82–88. (in Russian).
3. Gridchin V. A., Lubimsky V. M. Polysilicon Piezoresistor Geometry Effects on Their Strain-Sensitivity // «Actual Problems of Electronic Instrument Engineering» APEIE-2004: Proceedings of VII International Conference, Novosibirsk, 22–25.09, 2004. Novosibirsk: NSTU Press, 2004. V. 2, pp. 5–11. (in Russian).
4. Gridchin V. A., Gridchin A. V., Bunzina V.Yu. Lateral Nano-Piezoresistor Strain-Sensitivity // Materials of IX International Conferemce on Actual Problems of Electronic Instrument Engineering APEIE-2008, V. 2, 24–26.09, Novosibirsk, NSTU Press, 2008, pp. 11–14.
5. Gridchin V. A., Lubimsky V. M. Physico-Technological Problems of Polysilicon Tensoresistive Pressure Sensors Formation. Devices, No. 6 (60), pp. 23–27, 2005. (in Russian).
6. Lenk A., Electromechanische Sisteme, VEB-Verlag Technick, Berlin, 1975, Bd.3, 226 s.
7. Gridchin V. A. FEM Simulation of Piezoresistive Pressure Module / V. A. Gridchin, M. A. Chebanov // International School and Seminar on Modern Problems on Nanoelectronics, Micro- and Nanosystem Technologies Proceedings INTERNANO-2009: NSTU, Novosibirsk, Russia — October 28–31, 2009. — P. 44–46.
8. Lubimsky V. M. Design and Technology of Pressure ITP on the Basis of Polycrystalline Silicon Layers. // Thesis for Doctor of Technical Sciences, Novosibirsk, NSTU, 2005. (in Russian).
9. Toriyama T., Tanimoto Y., Sugiyama S. — Single crystalline silicon nano-wire piezoresistors for mechanical sensors — Transducers 01, Solid State Sensors and Actuators, Munich, Germany, June 10–14, (2001), 100 s.